MAGNETIC DESIGN OF THE DIPOLE MAGNETS FOR THE DIAMOND SYNCHROTRON SOURCE

N.Marks, J.A.Clarke, and D.J.Holder,
ASTeC, CLRC Daresbury Laboratory, Warrington, WA4 4AD, U.K.

Abstract

This paper presents the current design of the dipole magnets for the 3 GeV synchrotron source, DIAMOND. As final engineering details of the magnets will be decided by the manufacturer, working to a performance specification, this paper concentrates on the magnet geometry which will determine the magnetic performance of the dipoles; these details will be prescriptively specified. The paper details field modelling carried out in both two and three dimensions and the magnetic geometry determined in the transverse and longitudinal planes to meet the magnetic specification.

1 INTRODUCTION

The new U.K. synchrotron radiation source, DIAMOND, is being constructed by the private sector company 'DIAMOND Light Source Ltd', with the accelerator design being led and carried out by CLRC at its Daresbury Laboratory. The 3 GeV storage ring will have a 24 cell lattice containing 48 dipole magnets, 240 quadrupoles and 168 sextupoles. The dipoles will generate a field of 1.4 T at the 3 GeV operating level and will be curved, parallel ended 'C type' magnets, with the gap opening on the inside of the ring, to provide access for vacuum pumping.

2 SPECIFICATION

2.1 Dipole Parameters

Beam dynamic investigations [1] have defined the beam stay clear and good field apertures in the dipole whilst vacuum vessel design has indicated the space required for wall thickness and tolerances. These data, together with the resulting gap, are given in Table 1.

Table 1: Aperture provisions in the dipole

horizontal beam aperture	± 12 mm
vertical beam aperture	± 15 mm
vessel assembly tolerances	± 3 mm
wall thickness : 2 x 5 mm	10 mm
pole shims: 2 x 0.3 mm	0.6 mm
total magnet gap at pole centre	46.6 mm

The resulting dipole parameters are given in Table 2.

Table 2: Dipole Parameters

number of dipoles	48
physical length	0.900 m
required magnetic length	0.935 m
induction at beam	1.4 T
beam radius of curvature	7.16 m
magnet configuration	C core, parallel ends
good field full aperture (h x v)	24 mm x 30 mm
good field quality (ΔB/B)	± 0.01 %

2.2 Magnet Steel

A standard steel used extensively for d.c. accelerator magnets, where low field performance is not critical, is 'Stabocor' 1300-100A, a low carbon, medium silicon 1 mm sheet material. The B/H figures for this steel are made available by the manufacturers and these have been used as a basis for the non-linear modelling. To provide for variations from commercial suppliers, the magnetic field (H) specified for each value of induction (B) has been increased by 5% above the published value. These figures have been used for the f.e.a. simulations. The resulting permeability curves, parallel and normal to the steel rolling directions, are shown in Fig 1.

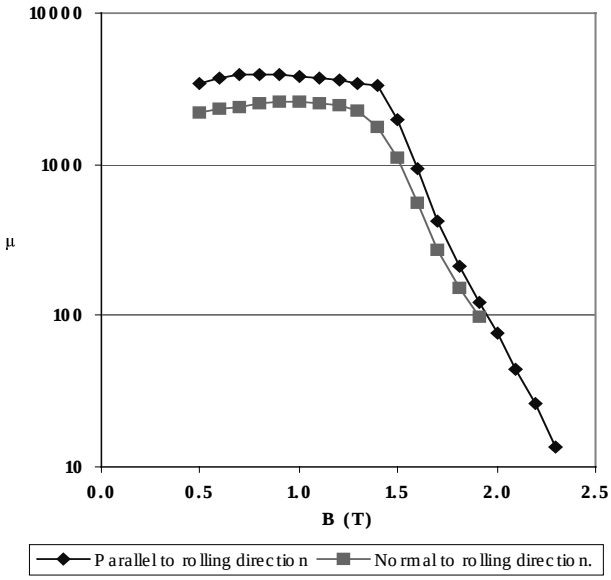

Figure 1 Variation in relative permeability (μ) with flux density (B) used for non-linear finite element analysis of the dipoles.

3 DIPOLE TRANSVERSE GEOMETRY

3.1 Magnet Geometry

Using the two-dimensional, non-linear, finite element magneto-static code OPERA 2D, a pole and yoke geometry was developed for the dipole which met the operational requirements for the magnet. The steel in the pole and back-leg was modelled using the 'parallel to rolling direction' magnetisation curve, whilst the top and bottom yokes had 'normal to rolling direction' properties imposed. The pole face had a broad, low shim at the pole edge, to maintain the field homogeneity over the required horizontal aperture. Outside the shims, the pole was terminated by a Rogowski roll-off, followed by a linear taper to the pole root. Parameters for the pole are given below in Table 3. The dipole will be curved, to follow the path of the circulating beam, so it is not necessary to increase the radial aperture of the magnet to accommodate any beam sagitta.

Table 3: Pole data used for dipole model.

x (mm)	y (mm)	Description
0.0	23.300	Centre of upper pole
26.0	23.300	Shim commences
34.0	23.030	
36.0	23.000	Start of full-height shim
38.0	23.000	End of shim
42.0	23.253	Start of Rogowski roll-off
46.0	23.587	
50.0	24.032	
54.0	24.621	
58.0	25.402	
62.0	26.439	
66.0	27.815	
70.0	29.640	End of Rogowski roll-off
84.0	93.000	End of pole taper
84.0	128.000	Pole corner (symmetrical)

Yoke dimensions were:

- top and bottom yoke: 250 mm;
- back-leg: 240 mm.

The coil design was based on the parameters in Table 4.

Table 4: Coil parameters

minimum amplitude linearity	97%;
required total Amp-turns at 1.4 T	53,474 At
no. of turns (total per magnet)	40
operating current at 1.4 T	1,337 A
current density in copper	4 A/mm^2
conductor cross section	334.2 mm^2
conductor dimensions	20 mm x 18.6 mm
water cooling tube diameter	7 mm
temperature rise in cooling water	10 ° C
number of pancakes	4
turns per pancake (2 layers of 5)	10

The chosen current density of 4 A/mm^2 in the copper conductor represents a rough optimum between lifetime operational costs of the facility and the initial capital cost.

3.2 Predicted Field Quality

The predicted homogeneity in vertical field along the x axis ($\Delta B_y(x)/B_y(0)$) is shown in Fig 2.

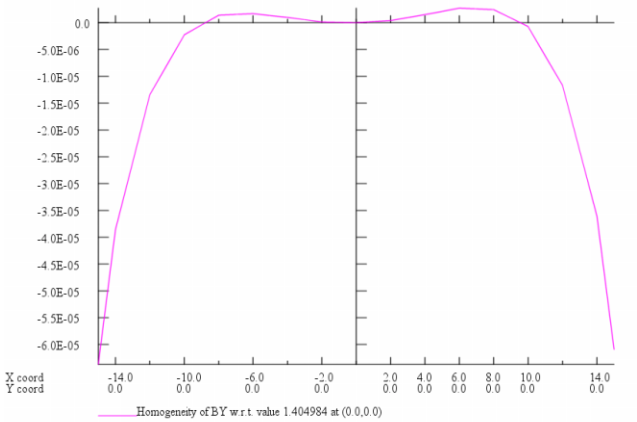

Figure 2: Non-linear prediction of field homogeneity ($\Delta B_y(x)/B_y(0)$) on y = 0 axis at the field level of 1.4 T; co-ordinates in mm.

Fig 2 indicates the following homogeneity:

- $\Delta B_y(x)/B_y(0)$ = + 0.0005 % x = 7 mm;
- $\Delta B_y(x)/B_y(0)$ = 0 x = 9 mm;
- $\Delta B_y(x)/B_y(0)$ = - 0.007 % x = 15 mm.

The homogeneity in the x, y plane, is displayed in Fig 3. This shows contour lines of ± 0.01% in ($\Delta B_y(x)/B_y(0)$); the shaded rectangle indicates the required good field region in the transverse plane.

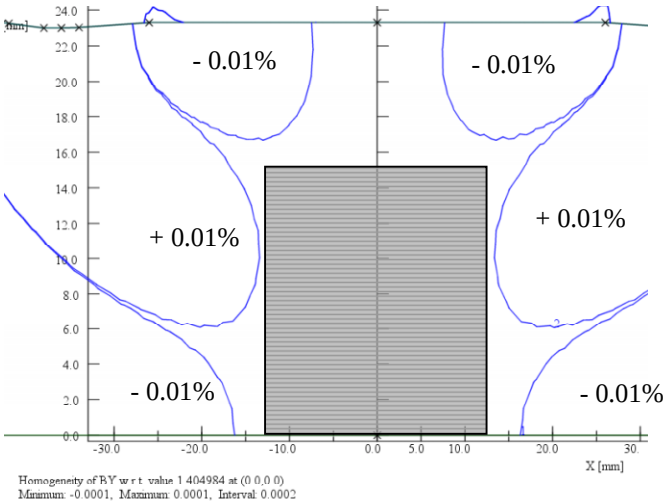

Figure 3: Field homogeneity at 3 GeV in half the transverse plane indicated by contours of ± 0.01% in $\Delta B_y(x)/B_y(0)$; the shaded rectangle indicates the good field region of ± 12 mm horizontal, ± 15 mm vertical.

4 THREE-DIMENSIONAL MODELLING

4.1 *Magnet Geometry in Three Dimensions*

The magnet ends must be shaped in the azimuthal direction, with a 'roll-off' which smoothly increases the gap. This eliminates the sharp corner, which would lead to non-linear behaviour. To simplify the engineering, a roll-off geometry which followed a single longitudinal curve normal to the magnet end face was adopted. This would have no variation in the transverse plane. A Rogowski curve was used:

$$y = (g/2) + (g/\pi) \exp((\pi (z+a)/g) - 1)$$

where:
z is the position with respect to the magnet end (z = 0);
g = is the 'pseudo' gap to meet the pole at finite z;
a adjusts the roll-off position longitudinally.

The magnet was modelled in three dimensions using the non-linear finite element magneto-static code TOSCA; results were compared with the two-dimensional simulations and provided detail of the end field distribution. The three-dimensional model of the dipole is shown in Fig 4, with the coils excluded for clarity. This has identical geometry to the current engineering layout, with the exception that the model is straight, not curved.

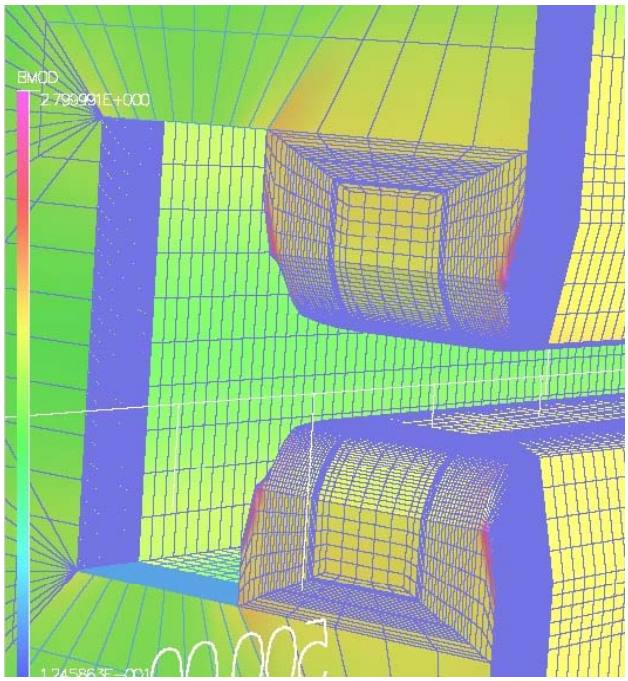

Figure 4: Three-dimensional dipole yoke, showing the end profile arrangements and finite element analysis grid used for non-linear field prediction.

4.2 *Field Quality Predicted by 3D Model*

A non-linear simulation, using the same magnetisation data for the steel as was used for the two-dimensional modelling, showed good agreement; the homogeneity prediction is shown in Fig 5.

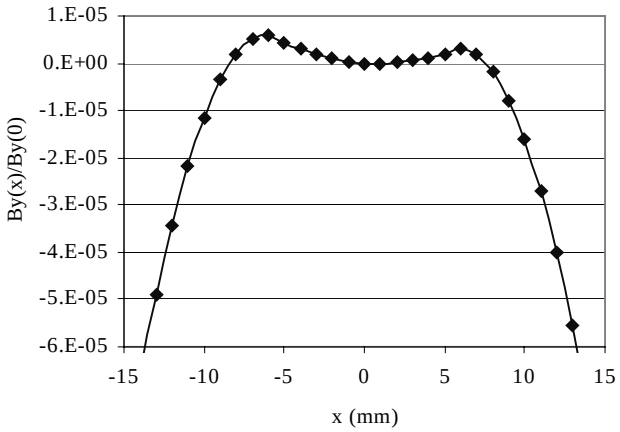

Figure 5: Non-linear prediction from three-dimensional model of field homogeneity ($\Delta B_y(x)/B_y(0)$) on y = 0 axis.

To estimate the dipole's field length, the distribution of the vertical flux was integrated through the length of the magnet, predicting a magnetic length of 931.7 mm.

With the un-shimmed roll-off, a negative sextupole component is generated at the dipole ends. To assess the magnitude of this, vertical flux densities were integrated azimuthally through half the magnet at different horizontal positions; the resulting variation in integrated field across the good field aperture is shown in Fig 6.

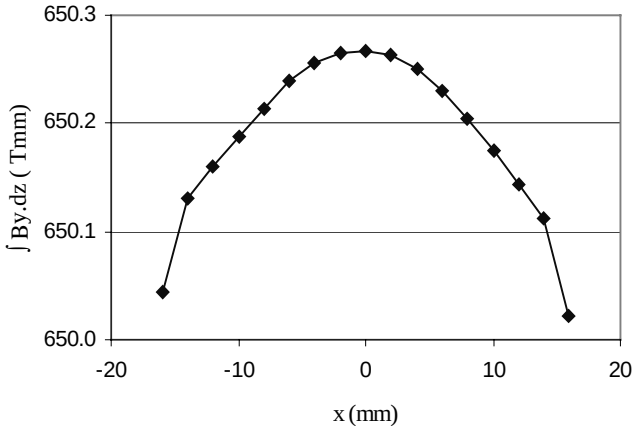

Figure 6: Homogeneity in the azimuthal integration through half the dipole of the vertical induction (B_y), against horizontal position (x).

From the data of Fig 6, the integrated sextupole component, which is concentrated in the dipole ends, is calculated to be - 0.7 T/m. This should be compared to the maximum strength (coefficient) of lattice sextupole magnets, which is 82.5 T/m. Hence, the estimated negative sextupole field at each dipole end resulting from a pole roll-off with no transverse shims is less than 0.5 % of the strength of the lattice sextupoles and can therefore be easily compensated by these elements.

5 REFERENCES

[1] N. Wyles et al "Defining the DIAMOND Storage Ring Apertures", these proceedings.